ELSEVIER

Biophysical Chemistry 122 (2006) 215–220

Biophysical Chemistry

http://www.elsevier.com/locate/biophyschem

A density functional theory study on the role of His-107 in arylamine *N*-acetyltransferase 2 acetylation

Qing-An Qiao [a,*], Chuanlu Yang [b], Rongjun Qu [a], Yueqing Jin [c], Meishan Wang [b], Zhihong Zhang [b], Qi Xu [a], Zhongxi Yu [a]

[a] *School of Chemistry and Materials Science, Yantai Normal University, Yantai 264025, China*
[b] *Department of Physics, Yantai Normal University, Yantai 264025, China*
[c] *Library of Yantai Normal University, Yantai, 264025, China*

Received 9 January 2006; received in revised form 17 March 2006; accepted 19 March 2006
Available online 27 March 2006

Abstract

Arylamine *N*-acetyltransferases (NATs, EC 2.3.1.5) catalyze an acetyl group transfer from acetyl coenzyme A (AcCoA) to primary arylamines, and are responsible for the biotransformation and metabolism of drugs, carcinogens, etc. Structure analysis revealed that His-107 was likely the residue accountable for mediating acetyl transfer. We have examined the full catalytic mechanism of this system by means of DFT method. The results indicate that if the acetyl group directly transferred from the donor, *p*-nitrophenyl acetate, to the acceptor, cysteine, the high activation energy will be a great hindrance. These energies have dropped a little in a range of 20–25 kJ/mol when His-107 is assisting the transfer process. However, when protonated His-107 is mediating the reaction, the activation energies have dropped about 70–85 kJ/mol. Our calculations strongly support an enzymatic acetylation mechanism that experiences a thiolate–imidazolium pair, which have verified the presumption from experiments.

Keywords: Arylamine *N*-acetyltransferase 2; Density functional theory; Acetyl transfer; Role of His-107

1. Introduction

The arylamine *N*-acetyltransferases (NATs, EC 2.3.1.5) NAT1 and NAT2 are phase II metabolism enzymes, which catalyze the transfer of an acetyl group from AcCoA to the nitrogen or oxygen atom of primary arylamines, and hydrazines, as well as their *N*-hydroxylated metabolites [1]. Most of the substrates for NATs are arylamine carcinogens (e.g. 2-aminofluorene, 4-aminobiphenyl, etc.) and xenobiotics, so that a number of the metabolites are electrophilic that are considered to be the ultimate carcinogens responsible for DNA adduct formation [2,3]. Much effort has been done to quantify the potential toxicological risks of exposure to the arylamine carcinogens by genetic and epidemiological studies of NAT polymorphisms [3,4]. To humans, the two functional NAT isozymes, NAT1 and NAT2, show great differences in substrate specificity and tissue distribution in spite of 81% amino acid sequence identity [5]. The latter, NAT2, is expressed predominantly in liver and intestinal epithelium [6].

Previous studies [2,7,8] have revealed that NATs catalyze an acetyl transfer by a classical ping-pong kinetic mechanism, in which an active site cysteine is first acetylated by formation of an acetyl–enzyme intermediate, and the acetyl group is subsequently transferred to the arylamine in the second half-reaction. Site-directed mutagenesis analysis of human NAT2 and *Salmonella typhimurium* NAT (StNAT) suggested that a cysteine residue in the active site (Cys-68 or Cys-69) were responsible for mediating the acetylation process [7,8]. Furthermore, the X-ray structures of StNAT and *Mycobacterium smegmatis* NAT have demonstrated a catalytic triad composed of Cys-69, His-107, and Asp-122 (Fig. 1) [9], and this catalytic triad is strictly conserved across all known NATs. A recent pre-steady state and steady state kinetic studies on *p*-nitrophenyl acetate (PNPA) and NAT2 revealed that the catalytic mechanism of NAT2 depends on the formation of a thiolate–imidazolium pair [10,11]. The required steps in the first half of acetylation reaction include the transfer of an acetyl group

* Corresponding author. Tel.: +86 535 6672176; fax: +86 535 6672574.
E-mail addresses: qiaoqa@hotmail.com, qiaoqa@sdu.edu.cn (Q.-A. Qiao).

0301-4622/$ - see front matter © 2006 Elsevier B.V. All rights reserved.
doi:10.1016/j.bpc.2006.03.011

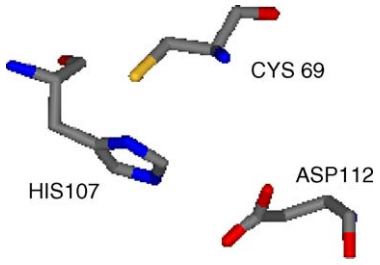

Fig. 1. X-ray structures of StNAT active site.

from the acetyl donors, *p*-nitrophenyl acetate (PNPA), to the active site cysteine residue, together with a removal of one proton from cysteine to PNPA. Though much effort has been done on the catalytic mechanism of this enzymatic system, it is unknown whether these steps occur concertedly or not [12–14]. What's more, what roles the active center site residues play is controversial and further research is still needed both experimentally and theoretically [15].

In this paper, we have examined different pathways for acetyl transfer process from the donor, PNPA, to the substrate, cysteine, which structures are shown in Fig. 2. Three different mechanisms (Fig. 3) are calculated as following: (1) the direct acetyl transfer from PNPA to cysteine (**Mech. 1**); (2) the His-107 assisted acetyl transfer reaction (**Mech. 2**); (3) the protonated His-107 mediating acetyl transfer process (**Mech. 3**). Due to the fact that the biological activity of Histidine mainly depends on its imidazole structure, we employed imidazole molecule as a simplified model. Such treatment has been proved effective and successfully performed on a number of enzymatic systems [16,17].

2. Methodology

The full catalytic mechanisms of this model system are examined by the hybrid density functional theory (DFT) B3LYP [18] as implemented in Gaussian03 program package [19], which method has previously been successfully employed on a number of enzymatic reactions [20]. The inherent accuracy of the B3LYP method can be estimated from benchmark tests [21], in which the average error in the atomization energies of the G2 set, consisting of 55 small first- and second-row molecules, is found to be 2.2 kcal/mol. When the 6-31G* and 6-311+G (3df, 2p) basis sets were used, the B3LYP hybrid functional was much preferred to the Hartree–Fock (HF) and MP2 methods. The average deviation for bond lengths is less than 0.02 Å, and for angles and dihedrals less than 1°. Of course, the DFT method is not perfect and sometimes fails in treatment of dispersion-rich interactions, however, it is successfully applied on many biological systems [22,23].

The structures of all reactants, intermediates, transition states and products are fully optimized at B3LYP/6-31G* level of theory. The most stable conformations as well as their energies at every equilibration and transition states have been figured out. Frequency calculations have been performed to all stationary points. The transition states have been identified by analyzing their vibrational modes and each has only one imaginary frequency. Finally, MP2/6-31+G** method is employed on the optimized structures of stationary points to get more accurate energy profiles. If not specially pointed out, all the following energy analyses refer to the results from MP2/6-31+G**//B3LYP/6-31G* calculations.

3. Results and discussion

3.1. *Mech. 1*: direct acetyl transfer between PNPA and cysteine

In **Mech. 1**, the His-107 residue is not involved through the whole process. The Natural Population Analysis (NPA) [24] for the reactants suggests that both O6 and O7 are electronegative (−0.568 and −0.544 respectively) and each of them can be easily attacked by a proton. Such a structure will lead to two different pathways for the acetyl transfer: **path a** and **path b**. In the former, the migration of acetyl group can be achieved via two following steps: firstly, the proton H3 migrates to O6 generating intermediate **Int1** via transition state **1ts1**, then a second migration from O6 to O7 via transition state **1ts2** will direct to the products. **path b** is a concerted reaction pathway, in which the transfer of acetyl group from O7 to S2 and the migration of H3 to O7 will take place simultaneously. The main structure data of all the reactants, intermediates and transition states have been listed in Table 1.

3.1.1. *Path a*

In the stepwise pathway **path a**, the first migration of H3 will lead to transition state **1ts1**. The planar sp2 hybridization of C5 now tends to tetrahedral sp3 hybridization. As O6 is attacked by H3 atom, the bond length of C5–O6 is getting 0.093 Å longer increasing its single bond character. According to the NPA of **1ts1**, the natural charge on H3 is 0.470 while O6 has higher negative charge of −0.705, and they are inclined to form a covalent bond

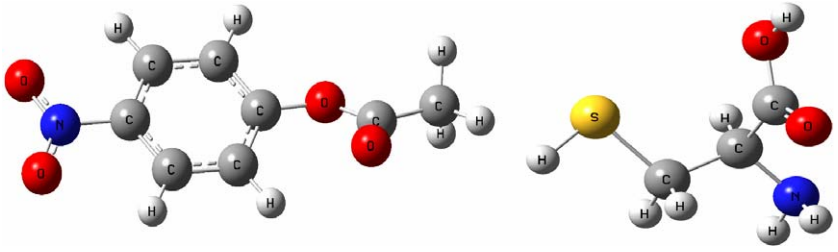

Fig. 2. Structures of the acetyl donor PNPA and the acceptor cysteine.

with each other. The only imaginary frequency of **1ts1** is 531.5i cm^{-1}, with the energy barrier as high as 159.0 kJ/mol.

After the successful transfer of H3 atom, intermediate **Int1** is located on the Potential Energy Surface (PES). The double bond of C5–O6 has converted to a single bond completely. Wang et al. [11] have proposed several mechanistic options for NAT2 acetylation, all of which experienced a tetrahedral intermediate, a thiol ester as **Int1**. Our calculations have verified this presumption, and suggested that **Int1** is short-lived as a local minimum on the PES, and will lead to a subsequent proton transfer process capable of producing a new transition state **1ts2**. For **1ts2**, the bond length of C5–O7 is stretched to 2.179 Å indicating a very weak covalence and little orbitals overlap between them. The small degree of dihedral H3O6C5O7 (−8.2°) indicates the four-membered ring composed of C5, O6, H3 and O7 is nearly planar, which makes it possible for the neighbour atoms have their orbitals overlapped to a full extent. In the mean time, the strong stress resulted from the small angle degrees of about 80° for O6C5O7 and O6H3O7 will give rise to great instability for this system. The complete rupture of this four-membered ring will direct to the final products.

3.1.2. *Path b*

In the concerted **path b**, **1ts3** is the only transition state to connect the reactants and products. C5 begins to show some characters of sp3 hybridization when attacked by S2. Simultaneously, the bond length of S2–H3 has been elongated from an equilibrium value of 1.350 to 1.529 Å and is nearly to break. The distance between C5 and S2 is 2.387 Å, suggesting their orbitals overlapped with each other through a weak covalent bond now. Similar to **1ts1** and **1ts2**, there is a four-membered ring with strong stress in **1ts3**'s structure as well. But the energy barrier for **1ts3** is as high as 195.7 kJ/mol, which is 36.7 kJ/mol and 56.1 kJ/mol higher than those of **1ts1**'s and **1ts2**'s respectively. H3 is the most reactive atom and vibrates the most intensively according to the normal vibrational modes analysis. The only imaginary frequency for **1ts3** is 1083.6i cm^{-1}.

In principle, the acetyl transfer can be accomplished via both **path a** and **path b**, but **path a** is much favored to **path b** in the competition due to its lower activation energy costs. For **Mech. 1**, all the three transition states have a four-membered ring with strong stress, in which the proton being transferred is the most active.

3.2. *Mech. 2: the His-107 assisted acetyl transfer reaction*

Previous studies [9–11] have supposed that His-107 might play a key role in the acetyl transfer reaction, but how it works in the catalysis keeps unclear. Based on the experimental studies, we have provided a detailed study of His-107 (nonprotonated **Mech. 2**, protonated **Mech. 3**) assisted acetylation process.

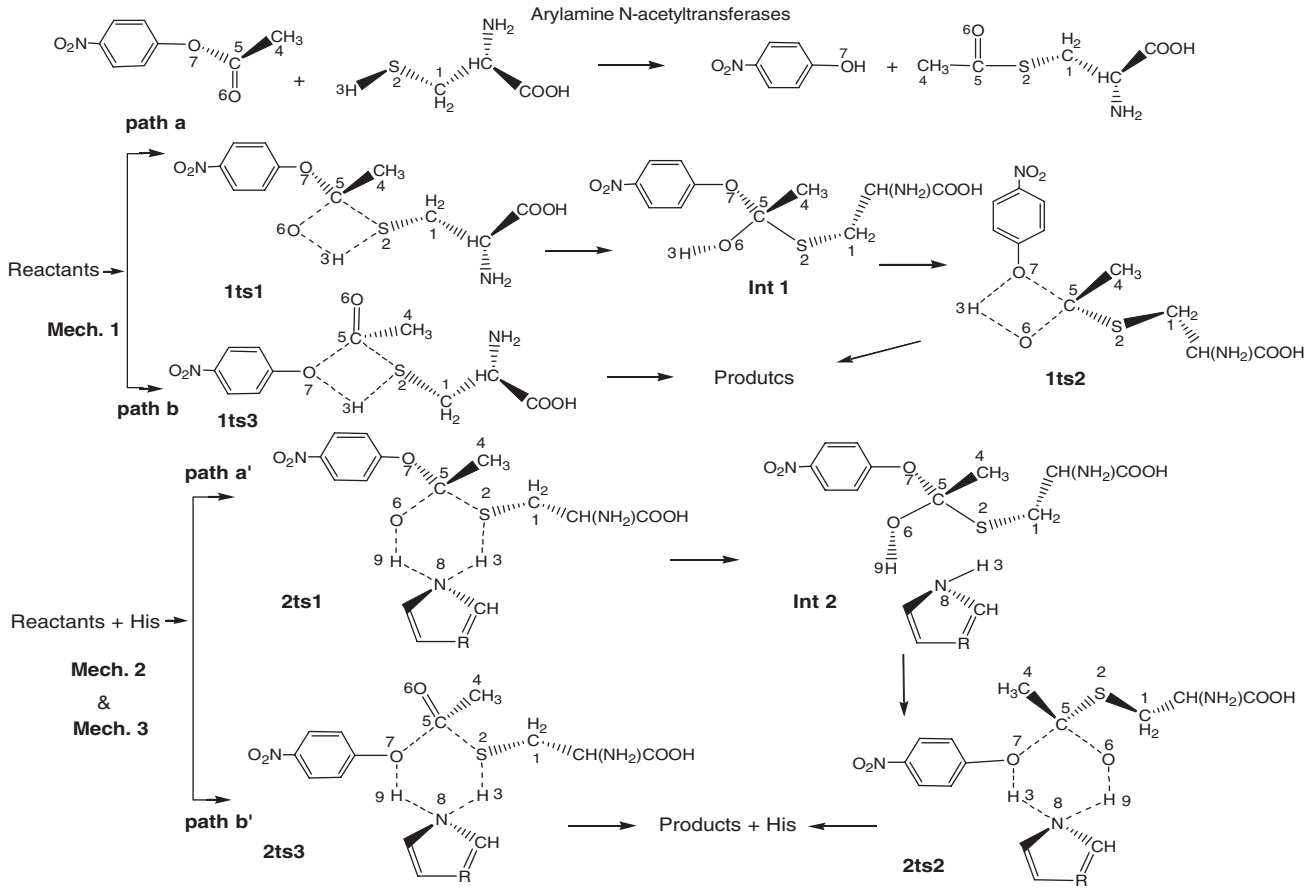

Fig. 3. The different reaction paths together with the structures of transition states and intermediates (in **Mech. 2**, R═N. In **Mech. 3**, R═NH^+, and the corresponding pathways are marked as **path a″** and **path b″**, transition sates and intermediate as **3ts1**, **Int3**, **3ts2** and **3ts3**).

Table 1
The main structure data of the stationary points together with their relative energies

	Reactants[a]	1ts1	Int1	1ts2	1ts3	2ts1	Int2	2ts2	2ts3	3ts1	Int3	3ts2	3ts3
Relative energy (kJ/mol)	0	159.0	39.4	139.6	195.7	138.1	20.6	114.8	170.7	85.8	−10.9	60.4	110.3
Bond length (Å)													
C1–S2	1.852	1.836	1.842	1.840	1.831	1.841	1.839	1.838	1.839	1.843	1.835	1.828	1.844
S2–H3	1.350	1.922	–	–	1.529	1.618	2.352	–	1.547	1.682	1.952	–	1.347
C4–C5	1.507	1.493	1.517	1.500	1.494	1.498	1.528	1.501	1.497	1.518	1.522	1.498	1.495
C5–O6	1.204	1.297	1.391	1.317	1.278	1.275	1.383	1.272	1.219	1.376	1.392	1.281	1.215
C5–O7	1.379	1.322	1.433	2.179	1.953	1.351	1.469	2.431	2.308	1.357	1.477	2.339	2.068
C5–S2		2.334	1.881	1.730	2.387	2.433	1.857	1.727	2.025	2.057	1.844	1.762	2.368
H3–O7			2.635	1.480	1.367	–	–	1.402	–	–	–	1.259	–
N8–H3						1.366	1.012	1.256	1.439	1.563	1.036	1.327	1.406
N8–H9						1.309	2.438	1.453	1.198	1.342	2.136	1.364	1.207
O6(O7)–H9						1.201	–	1.197	1.452	1.186	–	1.169	1.225
Bond angle (degree)													
H3S2C5		43.9			61.9	73.4			90.6	79.9			97.1
S2C5O6		76.5	111.2	119.8	112.7	93.6	107.3	120.2	115.7	101.5	108.2	125.7	121.2
O6C5O7		117.6	113.8	80.1	112.1	119.1	104.2	85.7	107.3	112.5	103.3	81.3	113. 7
S2(O7)H3N8						151.8	132.7	162.1	155.9	165.8	136.0	158.2	162.6
O6(O7)H9N8						163.8	122.6	161.0	158.1	162.9	125.8	167.2	163.2
H3N8H9						84.8	95.6	84.6	83.1	87.5	99.2	86.8	85.1
Dihedral (degree)													
H3O6(N8)C5S2(O7)		9.4		−8.2	9.6[b]	4.7		−2.9	2.5	6.4		−4.1	4.7
S2(O7)H3N8H9						−8.3		3.2	2.7	−9.7		2.4	3.5
C5O6(O7)H9N8						−77.2		78.9	−48.2	−65.7		68.1	−54.6
O6(O7)H9N8H3						36.3		−33.9	6.9	29.7		−35.1	1.7

[a] The energy sum of the reactants was taken as zero and the values in this column are gotten from the separated calculation results of the reactants.
[b] The degree of dihedral H3O7C5S2.

For imidazole, the HOMO mainly consists of the lone pair (−0.5412) of N8, which makes it easy for N8 to accept a proton from the donor and give one of its protons to the acceptor so as to assist to complete the acetylation. As well as **Mech. 1**, there are two different pathways for **Mech. 2** referred as **path a′** and **path b′**. The former is a stepwise one like **path a**, while the latter is concerted as **path b**.

3.2.1. *Path a′*

The stepwise **path a′** has experienced two sequential transition states named **2ts1** and **2ts2**. For **2ts1**, H3 atom is not directly migrating from S2 to O6 as in **path a**, but attacking N8 atom of His-107. The addition of this residue has changed the direct proton transfer way into an indirect one. The most obvious differences between **1ts1** and **2ts1** are derived from their structures. The latter is characterized by a six-membered ring (including S2, H3, N8, H9, O6 and C5 atoms) but not a four-membered ring as the former. From Table 1, one can easily find that transition state **2ts1** has two relatively large bond angles more than 150° (S2H3N8 and O6H9N8). Most of the energy savings has been achieved due to the loosen structure. The relative energy for **2ts1** is 138.1 kJ/mol, which is 13.1% decrease compared with **1ts1**, and as is the case for **2ts2** with the decrease of 17.8% when compared with **1ts2**. The results above are very similar to the water-assisted mechanism for Glycinamide Ribonucleotide Transformylase [25,26]. Whereas, from the 3D structures of **2ts1** and **2ts2** (Fig. 4), we find that the six-membered ring is not planar as Refs. [25,26], but looks more like in a chair conformation. Such a structure is considered to provide small stress and more stability to the transition state, which will finally result in low energy barrier for acetylation.

Int2 is the only intermediate through **path a′**, who is a H-bond binary complex. From our calculation, **Int2** is a thiolate–imidazolium pair as Ref. [11] suggested, because the total charge population for His-107 part is −0.185 and for the thiolate 0.185. The H-bonds, S2–H3 and H9–N8, are relatively weak according to the longer bond lengths of 2.352 and 2.438 Å respectively. The relative energy of **Int2** is 20.6 kJ/mol (Fig. 5), and it is a local minimum on the PES as **Int1**, but a little stable.

When residue His-107 is mediating the acetylation process, the two protons, H3 and H8, will migrate concertedly. In the six-

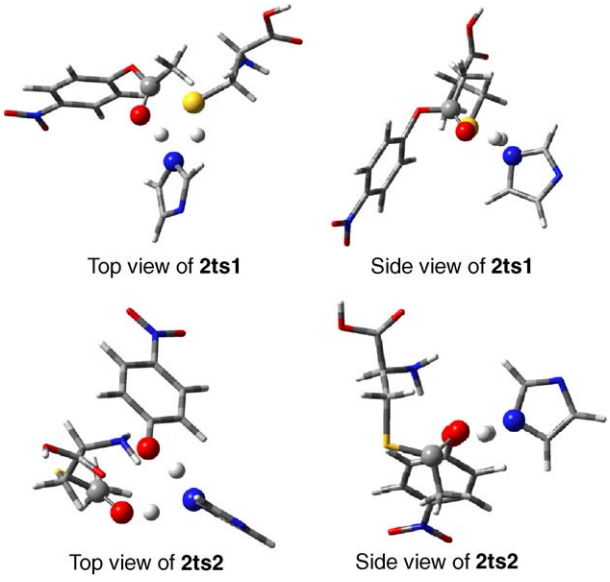

Fig. 4. The 3D structures of **2ts1** and **2ts2**.

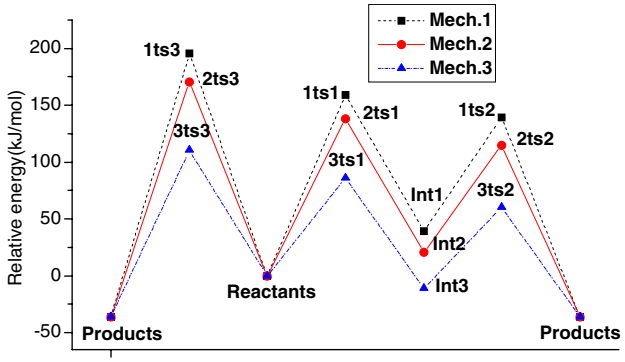

Fig. 5. The energy profiles of all the reaction paths.

membered ring, both of them have orbitals overlapped with their neighbour atoms, and the break of this ring will result in the target products. These conclusions are consistent with experimental results [11,15].

3.2.2. *Path b′*

2ts3 is the only transition state in **path b′**, in which there are two relative large angles, S2H3N8 and O7H9N8, more than 150° in the six-membered ring as well as **2ts1** and **2ts2**. The hybridizations of C5 and S2 for **2ts3** are similar to **1ts3**, but the energy barrier is getting 25.0 kJ/mol lower. The only imaginary frequency for **2ts3** is 880.6i cm^{-1}, and the two protons, H3 and H9, vibrated the most intensively. Obviously, the additional His-107 has made the molecular structure greatly relaxed so as to stabilize the transition state and reduce the relative energy, therefore, the acetylation process can be easily achieved.

For **Mech. 2**, the stepwise **path a′** is much preferable to the concerted **path b′** because of the lower energy barriers. His-107 can mediate the process by serving as a 'tunnel' that connects the donor and the acceptor for proton transfer. One proton is walking into the 'tunnel' while the other is leaving it at the same time. Though the one left is not the one entered, we can get the same products. The addition of His-107 stabilizes the transition states and substantially decreases the energy cost.

3.3. ***Mech. 3***: *the protonated His-107 mediating acetyl transfer reaction*

Duo to the fact that Histidine is very easy to be protonated and a pH-rate profile from experiments [11] reflects a decrease in the rate of acetylation, the protonated His-107 assisted acetyl transfer mechanism is studied in the following.

3.3.1. *Path a″*

When His-107 is protonated, the structure of the transition state **3ts1** shows a little variation compared with **2ts1**. H3 atom is 1.682 Å apart from S2 instead of 1.618 Å, while the distance between S2 and C5 has been reduced from 2.433 to 2.057 Å. As a result, S2 is greatly inclined to form a new bond with C5 and S2–H3 bond tends to break easily. When **3ts1** formed, the unit positive charge has been distributed at the whole system, mainly on the thiol-ester part (0.575), and makes the system more stable. The subsequent intermediate **Int3** is a protonated binary complex, which is more stable than **Int2** due to the stronger H-bonds interactions of S2–H3 (1.952 Å) and H9–N8 (2.136 Å). The situations for the second transition state **3ts2** are roughly the same as **3ts1** with 0.553 positive charges on thiol-ester part. The most obvious difference between **Mech. 2** and **Mech. 3** lies in the activation energies. The protonation of His-107 does not change the structures of the transition states greatly, e.g. the relaxed six-membered ring remained and the chair conformation is not destroyed, but brings great influence on the charge distribution. The energy barriers have been substantially decreased, for **3ts1**, the reduction is 73.2 kJ/mol and for **3ts2** 79.2 kJ/mol when compared with **Mech. 1**.

3.3.2. *Path b″*

Though His-107 is protonated, the six-membered ring structure remains in **3ts3**, and most of the positive charge (0.692) is mainly kept on His-107. When compared with **2ts3**, H3 is much closer to N8 while H9 approaches O7 with a much shorter distance, which means the concerted proton transfer process will be achieved with lower energy cost. In fact, the activation energy for **3ts3** has decreased from 195.7 to 110.3 kJ/mol with 43.6% reduction. However, it is still higher than those of **3ts1** and **3ts2**, and **path a″** is much preferable to **path b″** for acetylation reaction for **Mech. 3**.

The common character of all the three mechanisms is that all the concerted reaction pathways have higher activation energies than those of the stepwise ones. In other words, the participation of His-107, whether protonated or nonprotonated, can relax the transition states and lower the energy barriers in a different range, but can not change the priority of different pathways.

4. Conclusions

The following conclusions can be drawn from our calculations for catalytic system of NATs:

1) For three mechanisms, the energy barriers for the stepwise paths (**path a**, **path a′** and **path a″**) are lower than the concerted ones (**path b**, **path b′** and **path b″**), which indicates the stepwise paths are much favored. The participation of His-107 can not change the priority of different pathways. **path a″** is the much favored reaction path for acetyl transfer.
2) In **Mech. 1**, all the transition states have a four-membered ring structure, and the proton to be transferred (H3) is the most reactive atom. But in **Mech. 2** and **Mech. 3**, the four-membered ring has changed to a six-membered ring, which is not a plane but characterized by a chair conformation. It provides small stress and more stability for the transition state, and leads to lower energy barrier in the reaction pathway. The two protons (H3 and H9) to be transferred concertedly are the most reactive.
3) When His-107 mediating the reaction (**Mech. 2**), the energy barriers are lower than the corresponding ones in **Mech. 1** in a range of 20–25 kJ/mol. If His-107 is protonated (**Mech. 3**), the activation energies have dropped about 70–85 kJ/mol. It mediates the process by serving as a 'tunnel', accepting a proton from the donor and giving one of its protons to the acceptor simultaneously.

Our results show that the presumption of Ref. [11] is quite conceivable. There does exist a tetrahedral intermediate (**Int1**) or a thiolate–imidazolium pair (**Int2** or **Int3**) in the reaction pathway. Furthermore, the participation of His-107 in the transition state can loosen its structure and give a considerable relaxation to the unstable system. If it is removed, the higher energy barrier will make it hard to achieve the target products. It should be noticed that the effect of the other residues, including water molecules, in this reaction are out of consideration in the calculation. In an actual system, the whole reaction may be much easier to proceed due to the participation of other medium, and the energy barriers may be even lower than what we have calculated in **path a″**. Our results in this paper have well explained the presumption from experiments [11,15], and might be a valuable reference for further research in such field. A comprehensive molecule dynamics and a QM/MM study for the system are in process.

Acknowledgment

This work was supported by the Youth Natural Science Foundation of Yantai Normal University (No. 042902), the Youth Natural Science Foundation of Shandong Provincial Education Department (No.200139) and the National Natural Scientific Foundation of China (No. 10404030 and No. 20373071).

References

[1] P.E. Hanna, *N*-acetyltransferases, *O*-acetyltransferases, and *N*,*O*-acetyltransferases: enzymology and bioactivation, Adv. Pharmacol. 27 (1994) 401–430.
[2] P.E. Hanna, Metabolic activation and detoxification of arylamines, Curr. Med. Chem. 3 (1996) 195–210.
[3] G.N. Levy, W.W. Weber, Enzyme Systems That Metabolise Drugs and Other Xenobiotics,in: C. Ioaniddes (Ed.), John Wiley and Sons, New York, 2002, pp. 441–457.
[4] D.W. Hein, D.M. Grant, E. Sim, Update on consensus arylamine-acetyltransferase gene nomenclature, Pharmacogenetics 10 (2000) 291–292.
[5] D.M. Grant, M. Blum, M. Beer, U.A. Meyer, Monomorphic and polymorphic human arylamine *N*-acetyltransferases: a comparison of liver isozymes and expressed products of two cloned genes, Mol. Pharmacol. 39 (1991) 184–191.
[6] A. Upton, N. Johnson, J. Sandy, E. Sim, Arylamine *N*-acetyltransferases of mice, men, and microorganisms, Trends Pharmacol. Sci. 22 (2001) 140–146.
[7] J.M. Dupret, D.M. Grant, Site-directed mutagenesis of recombinant human arylamine *N*-acetyltransferase expressed in *Escherichia coli*. Evidence for direct involvement of Cys68 in the catalytic mechanism of polymorphic human NAT2, J. Biol. Chem. 267 (1992) 7381–7385.
[8] M. Watanabe, T. Sofuni, T. Nohmi, Involvement of Cys69 residue in the catalytic mechanism of *N*-hydroxyarylamine *O*-acetyltransferase of *Salmonella typhimurium*. Sequence similarity at the amino acid level suggests a common catalytic mechanism of acetyltransferase for *S. typhimurium* and higher organisms, J. Biol. Chem. 267 (1992) 8429–8436.
[9] J.C. Sinclair, J. Sandy, R. Delgoda, E. Sim, M.E. Noble, Structure of arylamine *N*-acetyltransferase reveals a catalytic triad, Nat. Struct. Biol. 7 (2000) 560–564.
[10] J. Sandy, A. Mushtaq, A. Kawamura, J. Sinclair, E. Sim, M. Noble, The structure of arylamine *N*-acetyltransferase from *Mycobacterium smegmatis*: an enzyme which inactivates the anti-tubercular drug, isoniazid, J. Mol. Biol. 318 (2002) 1071–1083.
[11] H. Wang, G.M. Vath, K.J. Gleason, P.E. Hanna, C.R. Wagner, Probing the mechanism of hamster arylamine *N*-acetyltransferase 2 acetylation by active site modification, sitedirected mutagenesis, and pre-steady state and steady-state kinetic studies, Biochemistry 43 (2004) 8234–8246.
[12] H.H. Andres, H.J. Kolb, R.J. Schreiber, L. Weiss, Characterization of the active site, substrate specificity and kinetic properties of acetyl-CoA: arylamine *N*-acetyltransferase from pigeon liver, Biochim. Biophys. Acta 746 (1983) 193–201.
[13] H.H. Andres, A.J. Klem, L.M. Schopfer, J.K. Harrison, W.W. Weber, On the active site of liver acetyl-CoA. Arylamine *N*-acetyltransferase from rapid acetylator rabbits (III/J), J. Biol. Chem. 263 (1988) 7521–7527.
[14] B. Riddle, W.P. Jencks, Acetyl-coenzyme A: arylamine *N*-acetyltransferase. Role of the acetyl-enzyme inter-mediate and the effects of substituents on the rate, J. Biol. Chem. 246 (1971) 3250–3258.
[15] H. Wang, L. Liu, P.E. Hanna, C.R. Wagner, Catalytic mechanism of hamster arylamine *N*-acetyltransferase 2, Biochemistry 44 (2005) 11295–11306.
[16] H. Fahmi, P.E.M. Siegbahn, Catalytic mechanism of glyoxalase I: a theoretical study, J. Am. Chem. Soc. 123 (2001) 10280–10289.
[17] P.L. Cummins, J.E. Gready, Energetically most likely substrate and active-site protonation sites and pathways in the catalytic mechanism of dihydrofolate reductase, J. Am. Chem. Soc. 123 (2001) 3418–3428.
[18] C. Lee, W. Yang, R.G. Parr, Development of the Colle–Salvetti correlation-energy formula into a functional of the electron density, Phys. Rev., B 37 (1988) 785–789;
A.D. Becke, A new mixing of Hartree–Fock and local density-functional theories, J. Chem. Phys. 98 (1993) 1372–1377;
A.D. Becke, Density-functional thermochemistry. III. The role of exact exchange, J. Chem. Phys. 98 (1993) 5648–5652.
[19] Gaussian 03, Revision B.05, M.J. Frisch, G.W. Trucks, H.B. Schlegel, G.E. Scuseria, M.A. Robb, J.R. Cheeseman, J.A. Montgomery, Jr., T. Vreven, K.N. Kudin, J.C. Burant, J.M. Millam, S.S. Iyengar, J. Tomasi, V. Barone, B. Mennucci, M. Cossi, G. Scalmani, N. Rega, G.A. Petersson, H. Nakatsuji, M. Hada, M. Ehara, K. Toyota, R. Fukuda, J. Hasegawa, M. Ishida, T. Nakajima, Y. Honda, O. Kitao, H. Nakai, M. Klene, X. Li, J.E. Knox, H.P. Hratchian, J.B. Cross, C. Adamo, J. Jaramillo, R. Gomperts, R.E. Stratmann, O. Yazyev, A.J. Austin, R. Cammi, C. Pomelli, J.W. Ochterski, P.Y. Ayala, K. Morokuma, G.A. Voth, P. Salvador, J.J. Dannenberg, V.G. Zakrzewski, S. Dapprich, A.D. Daniels, M.C. Strain, O. Farkas, D.K. Malick, A.D. Rabuck, K. Raghavachari, J.B. Foresman, J.V. Ortiz, Q. Cui, A.G. Baboul, S. Clifford, J. Cioslowski, B.B. Stefanov, G. Liu, A. Liashenko, P. Piskorz, I. Komaromi, R.L. Martin, D.J. Fox, T. Keith, M.A. Al-Laham, C.Y. Peng, A. Nanayakkara, M. Challacombe, P.M.W. Gill, B. Johnson, W. Chen, M.W. Wong, C. Gonzalez, and J.A. Pople, Gaussian, Inc., Pittsburgh PA, 2003.
[20] P.E.M. Siegbahn, R.A.M. Blomberg, Transition-metal systems in bio-chemistry studied by high-accuracy quantum chemical methods, Chem. Rev. 100 (2000) 421–437 (and references therein).
[21] W. Charles Bauschlicher Jr., A comparison of the accuracy of different functionals, Chem. Phys. Lett. 246 (1995) 40–44;
C.W. Bauschlicher Jr., A. Ricca, H. Partridge, S.R. Langhoff, Recent Advances in Density Functional Methods, Part II, World Scientific Publishing Company, Singapore, 1997.
[22] F. Richard, Ab initio quantum chemistry: methodology and applications, Proc. Natl. Acad. Sci. U. S. A. 102 (2005) 6648–6653.
[23] L.A. Curtiss, K. Raghavachari, P.C. Redfern, J.A. Pople, Assessment of Gaussian-3 and density functional theories for a larger experimental test set, J. Chem. Phys. 112 (2000) 7374–7383.
[24] A.E. Reed, L.A. Curtiss, F. Weinhold, Intermolecular interactions from a natural bond orbital, donor–acceptor viewpoint, Chem. Rev. 88 (1988) 899–926 (and references therein).
[25] Q. Qiao, Z. Cai, D. Feng, Y. Jiang, A quantum chemical study of the water-assisted mechanism in one-carbon unit transfer reaction catalyzed by glycinamide ribonucleotide transformylase, Biophys. Chem. 110 (2004) 259–266.
[26] Q. Qiao, Z. Cai, D. Feng, Quantum study on a new mechanism in one-carbon unit transfer reaction: the water-assisted mechanism, Chin. J. Chem. 22 (2004) 505–507.